433

Non linear analysis of a functionally graded square plate with two smart layers as sensor and actuator under normal pressure

M. Arefi[a] and G.H. Rahimi*

Department of Mechanical Engineering, Tarbiat Modares University, Tehran, Iran, 14115-143

Abstract. The present paper addresses the nonlinear response of a FG square plate with two smart layers as a sensor and actuator under pressure. Geometric nonlinearity was considered in the strain-displacement relation based on the Von-Karman assumption. All the mechanical and electrical properties except Poisson's ratio can vary continuously along the thickness of the plate based on a power function. Electric potential was assumed as a quadratic function along the thickness direction and trigonometric function along the planar coordinate. By evaluating the mechanical and electrical energy, the total energy equation can be minimized with respect to amplitude of displacements and electrical potential. The effect of non homogenous index was investigated on the responses of the system. Obtained results indicate that with increasing the non homogenous index, the displacements and electric potential tend to an asymptotic value. Displacements and electric potential can be presented in terms of planar coordinate system. A linear analysis was employed and then the achieved results are compared with those results that are obtained using the nonlinear analysis. The effect of the geometric nonlinearity is investigated by using the comparison between the linear and nonlinear results. Displacement-load and potential-load curves verified the necessity of a nonlinear analysis rather than a linear analysis. Improvement of the previous results (by the linear analysis) through employing a nonlinear analysis can be presented as novelty of this study.

Keywords: plate; mechanical properties; electrical properties; nonlinear; functionally graded material; piezoelectric; sensor.

1. Introduction

Smart materials have been discovered for the first time in India. Indian men have found new group of materials named "Ceylon Magnet". These materials have a tendency to absorb the tiny particles when heated. Quartz has been known as a first piezoelectric material. The piezoelectric effect and inversed piezoelectric effect have been introduced as two main principles which can be used in sensor and actuator applications, respectively. The piezoelectric effect is understood as the linear electromechanical interaction between the mechanical and the electrical components in a piezoelectric structure. The piezoelectric effect has been presented scientifically by Pierre and Jacques Curie in 1880. Piezoelectric structures are very applicable in the industrial systems. For example,

*Corresponding Author, Associate Professor, E-mail: rahimi_gh@modares.ac.ir
[a]arefi63@gmail.com

these structures can be used as sensor or actuator in various geometries such as disk, cylinders and shells. Derivation of the relation between the applied loads and displacement in a piezoelectric structure such as disk or diaphragm may be considered as an important subject especially when the plate undergoes large deformation. In order to control the distribution of the displacement or electric potential in a piezoelectric structure, functionally graded piezoelectric material (FGPM) can be used.

The properties of this material can vary continuously along the coordinate system. These materials have been created for the first time in laboratory by a Japanese group of the material scientists. For many advantageous properties, these materials can be used in the vigorous environments with abruptly gradient of the pressure and temperature. A comprehensive study of literatures can justify the purpose and novelty of this study.

Woo and Meguid (2001) investigated the nonlinear analysis of the functionally graded plates and shallow shells. They proposed an analytical solution for the coupled large deflection of the FG plates and shallow shells. Von Karman theory was employed for considering the large transverse deflection. GhannadPour and Alinia (2006) investigated the large deflection analysis of a rectangular FG plate based on the Von Karman theory for simulation of the large deflection. The solution was obtained using minimization of the total potential energy with respect to unknown parameters. The solution has directed authors to investigate the effect of non homogeneity on the stresses and deformations. Hui-Shen (2007) considered the nonlinear response of a FG plate due to heat conduction. It was assumed that the plate to be shear deformable. Higher order shear deformation theory was employed for analysis of the problem. Banerjee *et al.* (2008) presented the analytical and numerical solutions for the large deflection analysis of a cantilever beam with geometric nonlinearity. Adomian decomposition and shooting methods were employed for analysis of the nonlinear system as analytical and numerical methods, respectively. The obtained results using shooting method were compared with those results using Adomian decomposition method.

Allahverdizadeh *et al.* (2008) investigated the nonlinear behavior of thin circular FG plates. The analysis was assumed to be axisymmetric and solution was derived based on a semi-analytical approach. Ebrahimi and Rastgo (2008) investigated the free vibration of smart circular thin FG plate using the classical plate theory. The power function was employed for simulation of the material properties distribution along the thickness direction. Plate was composed of a FG layer and two FGP layers at top and bottom of that. The obtained results were verified by those obtained results from three dimensional finite element analyses. Malekzadeh and Vosoughi (2009) investigated the large amplitude vibration of composite beams on the nonlinear elastic foundation. The foundation was supposed that has cubic nonlinearity with shearing layer. Soufyane (2009) investigated the stability of the linearized non uniform timoshenko beam. Alinia and GhannadPour (2009) investigated the large deflection analysis of a rectangular FG plate with logarithmic distribution of material properties. Sarfaraz Khabbaz *et al.* (2009) investigated the nonlinear analysis of FG plates under pressure based on the higher-order shear deformation theory. The first and higher order shear deformation theories were employed to investigate the large deflection of FG plate. The effect of the thickness and non homogenous index were investigated on the distribution of the displacements and stresses. Khoshgoftar *et al.* (2009) investigated thermo elastic analysis of a FGP cylinder under pressure. It was assumed that all mechanical and electrical properties except Poisson ratio vary continuously along the thickness direction based on a power function.

Pressure influences on the vibration characteristics of piezoelectric circular micro diaphragm based pressure sensors were investigated theoretically and experimentally by M. Olfatnia *et al.* (2010).

The construction and performance of cantilever micro-dilatometer designed to directly monitor

transverse strain in electro active polymer specimens actuated by high voltage is investigated by Zyłka and Janus (2010).

A functionally graded piezoelectric rotating cylinder as mechanical sensor under pressure and thermal loads is investigated analytically by Rahimi *et al.* (2011) for evaluation of angular velocity of rotary devices.

Some useful basic equations for nonlinear analysis can be employed from classic textbook of mechanical engineering (Lai *et al.* 1999, Boresi 1993, Ugural 1981).

The present paper investigates the nonlinear analysis of a FGP square plate as a sensor or actuator in industrial application. This structure can be used as an adjustable and controllable system to define pressure in sensor usage or actuate micro positioner system in actuator usage.

2. Formulation

The nonlinear equations of a pressurized FG plate with the two smart layers are introduced in the present section. The classic plate theory (CPT) is employed for simulation of the displacements. Based on the CPT, the displacement of every layer is defined by two terms including the displacement of mid-plane and rotation about the mid-plane (Ugural 1981, Ebrahimi and Rastgo 2008). Therefore, we will have

$$\begin{cases} u(x,y,z) = u_0(x,y) - z\,\dfrac{\partial w(x,y)}{\partial x} \\[2mm] v(x,y,z) = v_0(x,y) - z\,\dfrac{\partial w(x,y)}{\partial y} \\[2mm] w(x,y,z) = w(x,y) \end{cases} \tag{1}$$

where, u_0, v_0, w are displacement components of the of the plate mid-plane ($z = 0$) and $\vec{u} = (u, v, w)$ is displacement vector. Considering Eq. (1), the nonlinear components of strains is obtained as (Lai *et al.* 1999)

$$\{\varepsilon\} = \frac{1}{2}\left\{\nabla\vec{u} + \nabla^T\vec{u} + (\nabla^T\vec{u})(\nabla\vec{u})\right\} \rightarrow$$

$$\varepsilon_{ij} = \frac{1}{2}\left(\frac{\partial u_i}{\partial x_j} + \frac{\partial u_j}{\partial x_i} + \frac{\partial u_k}{\partial x_i}\frac{\partial u_k}{\partial x_j}\right) \tag{2}$$

where, ε_{ij} are the strain components and ∇ is del operator. The nonlinear components of the strains are obtained using substituting Eq. (1) into Eq. (2) as follows

$$\varepsilon_{xx} = \frac{\partial u_0}{\partial x} - z\frac{\partial^2 w}{\partial x^2} + \frac{1}{2}\left(\frac{\partial w}{\partial x}\right)^2$$

$$\varepsilon_{yy} = \frac{\partial v_0}{\partial y} - z\frac{\partial^2 w}{\partial y^2} + \frac{1}{2}\left(\frac{\partial w}{\partial y}\right)^2 \tag{3}$$

$$\varepsilon_{xy} = \frac{1}{2}\left(\frac{\partial u_0}{\partial y} + \frac{\partial v_0}{\partial x} - 2z\frac{\partial^2 w}{\partial x\partial y} + \frac{\partial w}{\partial x}\frac{\partial w}{\partial y}\right)$$

As mentioned previously, the plate containing the piezoelectric layers (Fig. 1). Therefore, the constitutive equations for structures made of piezoelectric materials are expressed as (Khoshgoftar *et*
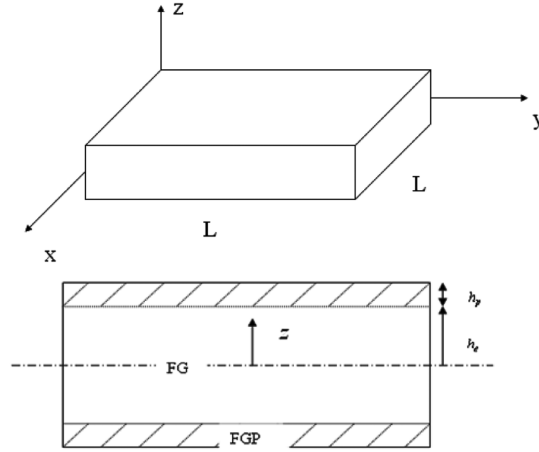
Fig. 1 The schematic figure of a FGP square plate

al. 2009)

$$\sigma_{ij} = C_{ijkl}\varepsilon_{kl} - e_{ijk}E_k \tag{4}$$

where, σ_{ij} and ε_{kl} are the stress and strain components, E_k is electric field, C_{ijkl} and e_{ijk} are the stiffness and piezoelectric coefficients. C_{ijkl} and e_{ijk} are the components of tensor of order 4 and 3 and in the general state have 81 and 27 components, respectively. Electric field E_k is obtained by a potential function $\phi(x, y, z)$ as follows (Khoshgoftar *et al.* 2009)

$$\phi = \phi(x, y, z) \rightarrow E_k = -\frac{\partial \phi(x, y, z)}{\partial k}, k = x, y, z \tag{5}$$

The electric displacement D_i in the electromechanical system is defined using the linear composition of the strain and electric field as (Khoshgoftar *et al.* 2009)

$$D_i = e_{ijk}\varepsilon_{jk} + \eta_{ik}E_k \tag{6}$$

where, η_{ik} are the dielectric coefficients which are the components of tensor of order 2 and in the general state have 9 components.

Due to small ratio of the plate thickness with respect to the length and width of the plate, the normal stress σ_{zz} and shear stresses σ_{xz}, σ_{yz} is ignorable. The constitute equations based on the plane stress condition for elastic solid sections of the plate (FG) $-h_e \le z \le h_e$ are expressed as

$$\begin{cases} \sigma_{xx} = C^e_{xxxx}\varepsilon_{xx} + C^e_{xxxy}\varepsilon_{xy} + C^e_{xxyy}\varepsilon_{yy} \\ \sigma_{yy} = C^e_{yyxx}\varepsilon_{xx} + C^e_{yyxy}\varepsilon_{xy} + C^e_{yyyy}\varepsilon_{yy} \\ \sigma_{xy} = C^e_{xyxx}\varepsilon_{xx} + C^e_{xyxy}\varepsilon_{xy} + C^e_{xyyy}\varepsilon_{yy} \end{cases} \tag{7}$$

The constitute equations for piezoelectric sections of the plate (FGP) $h_e < |z| \le h_e + h_p$ are expressed as

$$\begin{cases} \sigma_{xx} = C^P_{xxxx}\varepsilon_{xx} + C^P_{xxxy}\varepsilon_{xy} + C^P_{xxyy}\varepsilon_{yy} - e_{xxx}E_x - e_{xxy}E_y - e_{xxz}E_z \\ \sigma_{yy} = C^P_{yyxx}\varepsilon_{xx} + C^P_{yyxy}\varepsilon_{xy} + C^P_{yyyy}\varepsilon_{yy} - e_{yyx}E_x - e_{yyy}E_y - e_{yyz}E_z \\ \sigma_{xy} = C^P_{xyxx}\varepsilon_{xx} + C^P_{xyxy}\varepsilon_{xy} + C^P_{xyyy}\varepsilon_{yy} - e_{xyx}E_x - e_{xyy}E_y - e_{xyz}E_z \end{cases} \tag{8}$$

The electric displacement equations for the piezoelectric sections of the FGP plate $h_e \leq z \leq h_e + h_p$ are

$$
\begin{cases}
D_x = e_{xxx}\varepsilon_{xx} + e_{xxy}\varepsilon_{xy} + e_{xyy}\varepsilon_{yy} + \eta_{xx}E_x + \eta_{xy}E_y + \eta_{xz}E_z \\
D_y = e_{yxx}\varepsilon_{xx} + e_{yxy}\varepsilon_{xy} + e_{yyy}\varepsilon_{yy} + \eta_{yx}E_x + \eta_{yy}E_y + \eta_{yz}E_z \\
D_z = e_{zxx}\varepsilon_{xx} + e_{zxy}\varepsilon_{xy} + e_{zyy}\varepsilon_{yy} + \eta_{zx}E_x + \eta_{zy}E_y + \eta_{zz}E_z
\end{cases}
\tag{9}
$$

The energy per unit volume of the plate $\bar{u}$ is evaluated by

$$
\bar{u} = \tfrac{1}{2}\{\varepsilon^T \sigma - E^T D\} \rightarrow
$$
$$
\bar{u} = \tfrac{1}{2}\{\sigma_{xx}\varepsilon_{xx} + \sigma_{yy}\varepsilon_{yy} + 2\sigma_{xy}\varepsilon_{xy} - D_x E_x - D_y E_y - D_z E_z\}
\tag{10}
$$

By introduction of the potential energy, the total energy equation of the plate under uniform or non-uniform pressure is expressed by (Ugural 1981)

$$
U = \iint_A \int_{-(h_e+h_p)}^{(h_e+h_p)} \bar{u}(x,\,y,\,z)\,dz\,dx\,dy - \iint_A p(x,\,y)w\,dx\,dy
\tag{11}
$$

The energy equation can be divided for two different sections of the plate as follows:

$$
U = \iint_A \int_{-h_e}^{h_e} \tfrac{1}{2}\{\sigma_{xx}^e\varepsilon_{xx} + \sigma_{yy}^e\varepsilon_{yy} + 2\sigma_{xy}^e\varepsilon_{xy}\}\,dz\,dx\,dy +
$$
$$
2\iint_A \int_{h_e}^{h_e+h_p} \tfrac{1}{2}\{\sigma_{xx}^p\varepsilon_{xx} + \sigma_{yy}^p\varepsilon_{yy} + 2\sigma_{xy}^p\varepsilon_{xy} - D_x E_x - D_y E_y - D_z E_z\}\,dz\,dx\,dy
\tag{12}
$$
$$
-\iint_A p(x,\,y)w\,dx\,dy
$$

    The plate is fixed to four simply support edges and therefore, the displacements at four edges are considered zero. Furthermore the homogenous boundary conditions are considered for the electric potential (Ebrahimi and Rastgo 2008). The solution procedure may be continued with assumption of four fields for the displacements and electric potential. The sinusoidal function is employed for these assumptions as follows (GhannadPour and Alinia 2006, Alinia and GhannadPour 2009)

$$
u_0(x,y) = \sum_p \sum_q U_{pq} \sin\left(\frac{2p\pi x}{L}\right)\sin\left(\frac{(2q-1)\pi y}{L}\right)
$$
$$
v_0(x,y) = \sum_p \sum_q V_{pq} \sin\left(\frac{(2p-1)\pi x}{L}\right)\sin\left(\frac{2q\pi y}{L}\right)
$$
$$
w(x,y) = \sum_p \sum_q W_{pq} \sin\left(\frac{(2p-1)\pi x}{L}\right)\sin\left(\frac{(2q-1)\pi y}{L}\right)
\tag{13}
$$
$$
\phi(x,y,z) = f(z)\sum_p \sum_q \Phi_{pq} \sin\left(\frac{(2p-1)\pi x}{L}\right)\sin\left(\frac{(2q-1)\pi y}{L}\right)
$$

where, U_{pq}, V_{pq}, W_{pq} and Φ_{pq} describes the amplitudes of the displacement components and electric potential, p and q defines the number of the required sentences for definition of the four fields. In order to evaluation of the results and comparison between different results p, q are limited to one
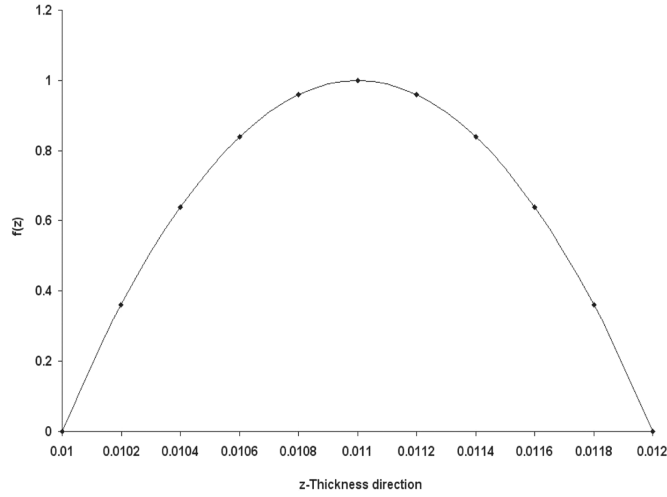
Fig. 2 The distribution of $f(z)$ along the thickness direction

(GhannadPour and Alinia 2006, Alinia and GhannadPour 2009). $f(z)$ guaranties this assumption that the electric potential at top and bottom of two piezoelectric layers must be zero. Therefore this function is (Ebrahimi and Rastgo 2008)

$$\phi(z = h_e) = \phi(z = h_e + h_p) = 0 \rightarrow f(z) = \left(1 - \left\{\frac{2z - 2h_e - h_p}{h_p}\right\}^2\right) \qquad (14)$$

Fig. 2 shows the assumed distribution for $f(z)$.

The energy equation is evaluated in terms of the displacements amplitude U_{pq}, V_{pq}, W_{pq} and electric potential Φ_{pq} as follows

$$U = U(U_{pq}, V_{pq}, W_{pq}, \Phi_{pq}) \qquad (15)$$

The solution of the system can be obtained by minimizing the energy equation (Eq. (15)) with respect to four amplitudes U_{pq}, V_{pq}, W_{pq}, Φ_{pq}.

$$R_i = \frac{\partial U}{\partial q_i} = 0, i = 1, 2, 3, 4, q_i = U_{pq}, V_{pq}, W_{pq}, \Phi_{pq} \qquad (16)$$

This minimizing tends to a system of algebraic nonlinear equations (Eq. (16)). The algebraic nonlinear equation can be solved and then final solutions of the system may be obtained analytically. The algebraic nonlinear equations can be solved by using the various analytical or numerical methods based on a computer program or package. Within these methods, solution by using the mathematical software is preferred. This preference is due to so much number of the nonlinear equations. Maple software is used for solution of the problem.

3. Results and discussion

3.1. Material properties

Before solution of the problem, it is appropriate to define the material properties for the FG and

FGP layers. For FG layer, it is assumed that the bottom of the plate is steel and top of that is ceramic. Therefore the distribution of the material properties for FG layer is (Ebrahimi and Rastgo 2008)

$$E(z) = (E_c - E_m)\left(\frac{1}{2} + \frac{z}{2h_e}\right)^n + E_m \quad -h_e \le z \le h_e \tag{17}$$

where, $E(z=-h_e)=E_m$, $E(z=h_e)=E_c$, $2h_e$ is thickness of elastic solid section of the plate and n is the non-homogenous index. The distribution of the mechanical and electrical properties for the two FGP layers can be supposed as a power function along the thickness direction as follows (Khoshgoftar *et al.* 2009)

$$E(z) = E_i\left(\frac{|z|}{h_e}\right)^n \quad h_e < |z| \le h_e + h_p \tag{18}$$

where, E_i represents the value of the all mechanical and electrical components at $|z| = h_e$ and h_e is thickness of the piezoelectric section. By these assumptions (Eqs. (17) and (18)), the energy equation can be obtained using Eq. (12). By minimization of the energy equation using Eq. (16), a set of nonlinear equations can be derived. The responses of the nonlinear equations can be evaluated using the Maple software.

The variable material properties of the FGP plate are selected as follows

$$\textit{Elastic solid section}: C^e_{xxxx} = C^e_{yyyy} = \frac{E_1(z)}{1-v^2}, C^e_{xxyy} = C^e_{yyxx} = \frac{vE_1(z)}{1-v^2}, C^e_{xyxy} = \frac{E_1(z)}{2(1+v)}$$

$$E_1(z) = (E_c - E_m)(\frac{1}{2} + \frac{z}{2h_e})^n + E_m \quad -h_e \le z \le h_e$$

$$\textit{Piezoelectric section}: C^P_{xxxx} = C^P_{yyyy} = \frac{E_2(z)}{1-v^2}, C^P_{xxyy} = C^P_{yyxx} = \frac{vE_2(z)}{1-v^2}, C^P_{xyxy} = \frac{E_2(z)}{2(1+v)}$$

$$E_2(z) = E_{h_e}(\frac{|z|}{h_e})^n \quad h_e \le |z| \le h_e + h_p$$

$$e_{xxx} = e_{yyy} = e_1(z), e_{xyy} = e_{yxx} = e_{zyy} = e_{zxx} = e_2(z), e_{xxy} = e_{yxy} = e_{zxy} = 0$$

$$\eta_{xx} = \eta_{yy} = \eta_{zz} = \eta_1(z), \eta_{xy} = \eta_{xz} = \eta_{yx} = \eta_{yz} = \eta_{zx} = \eta_{zy} = \eta_2(z)$$

$$e_1(z) = e_{1h_e}(\frac{|z|}{h_e})^n, e_2(z) = e_{2h_e}(\frac{|z|}{h_e})^n, \eta_1(z) = \eta_{1h_e}(\frac{|z|}{h_e})^n, \eta_2(z) = \eta_{2h_e}(\frac{|z|}{h_e})^n \quad h_e \le |z| \le h_e + h_p$$

where the numeric values for material properties and geometric parameters are (Ebrahimi and Rastgo 2008, Khoshgoftar *et al.* 2009)

$$E_c = 3.8 \times 10^{11} Pa, E_m = 2 \times 10^{11} Pa, E_{h_e} = 7.6 \times 10^{10} Pa$$

$$e_{1h_e} = 0.35 Cm^{-2}, e_{2h_e} = -0.16 Cm^{-2}, \eta_{1h_e} = 9.03 \times 10^{-11} C^2 N^{-1} m^{-2}, \eta_{2h_e} = 5.62 \times 10^{-11} C^2 N^{-1} m^{-2}$$

$$h_e = 10 \times 10^{-3} m, h_p = 2 \times 10^{-3} m, L = 0.2 m$$

Fig. 3 shows the distribution of the stiffness coefficient along the plate thickness for different values of non-homogenous index (n).

3.2 Evaluation of the results

This section deals with the most important results of the problem. By substituting the solution of the Eq. (16)(U_{pq}, V_{pq}, W_{pq}, Φ_{pq}) into Eqs. (7), (8) and (13), the mechanical and electrical components can be evaluated analytically or numerically.

The nonlinear behavior of the problem considered in Eqs. (2) and (3) can be understood carefully by plotting the mechanical and electrical components versus the normal applied pressure.

Fig. 4 shows the distribution of the maximum normal displacement in terms of the normal applied pressure. In this figure, increasing the normal pressure from 100 Mpa to 500 Mpa, increases the maximum displacement about 3.47 times of it's initial value.

Similar to Fig. 4, the distribution of the maximum electric potential is plotted versus the normal applied pressure in Fig. 5. The nonlinear distribution can be apparently understood in this figure.
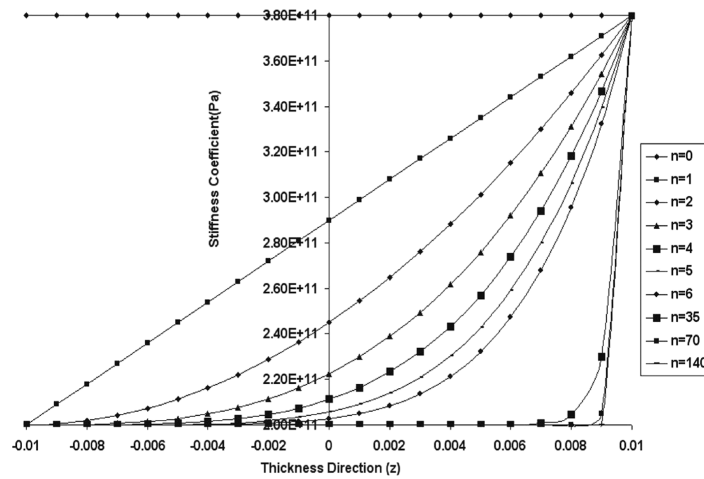

Fig. 3 The radial distribution of the stiffness coefficient along the thickness direction for different values of the non-homogenous indexes
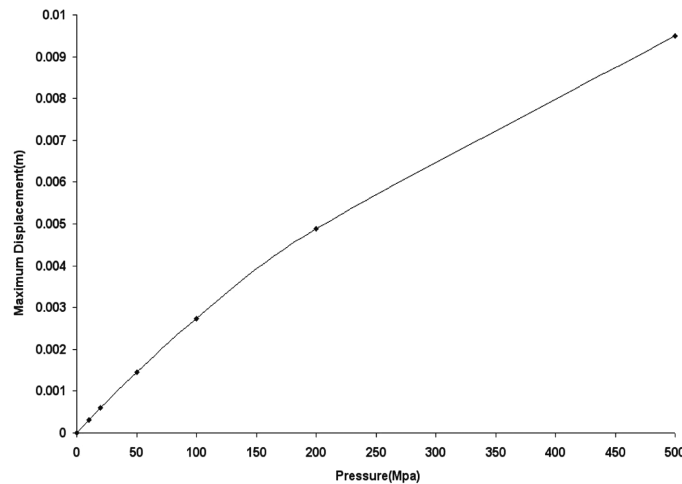

Fig. 4. The nonlinear distribution of the maximum displacement in terms of the normal applied pressure
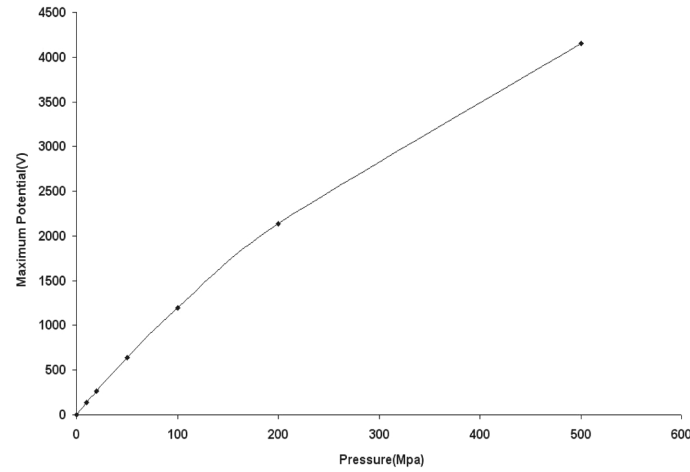
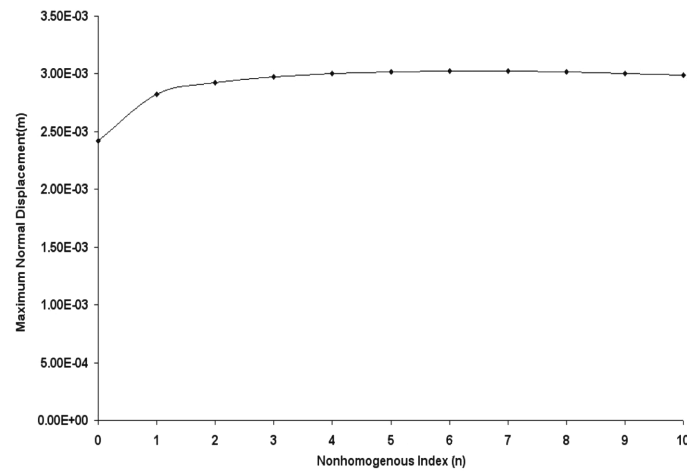Fig. 5 The nonlinear distribution of the maximum electric potential in terms of the normal applied pressure

Fig. 6 The distribution of the maximum value of the normal displacement in terms of non-homogenous index (*n*)

Solution procedure indicates that with increasing the non-homogenous index, the maximum value of the normal displacement tend to an asymptotic value. Fig. 6 shows the distribution of the maximum value of the normal displacement in terms of different values of the non-homogenous index (*n*).

By substituting the unknown amplitudes(U_{pq}, V_{pq}, W_{pq}, Φ_{pq}) derived from Eq. (16) into Eq. (7), the stress distribution of the plate mid-plane in terms of the various non-homogenous indexes can be obtained. Fig. 7 shows the distribution of the maximum stress in terms of the various non-homogenous indexes. Shown in Fig. 7 indicate that an asymptotic value is expected through increasing the non homogenous index (*n*).

Fig. 8 shows the distribution of the maximum electric potential in terms of the non-homogenous index (*n*). This figure is similar to Figs. 6 and 7 where the maximum electric potential tends to an asymptotic value with increasing the non-homogenous index. Fig. 9 shows the distribution of the maximum normal displacement for six values of the non-homogenous index versus the horizontal
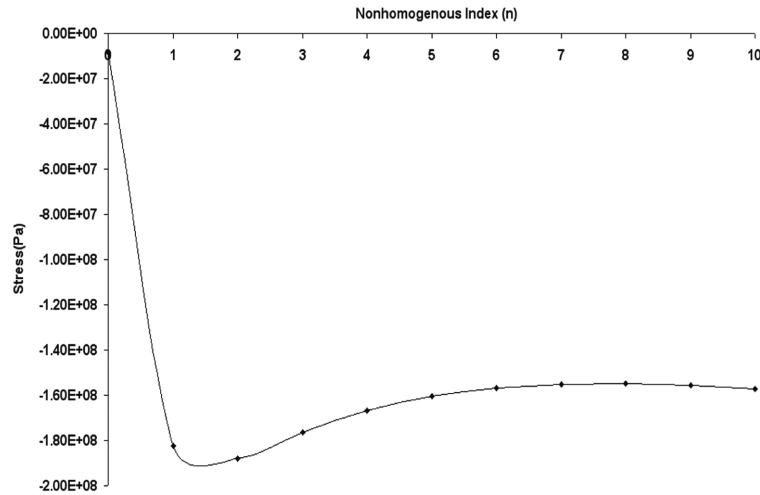
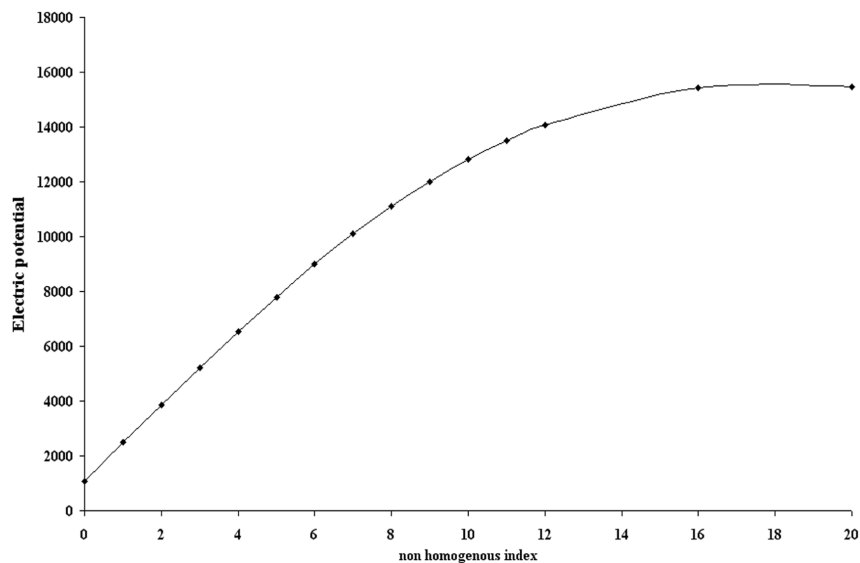Fig. 7 The distribution of the maximum value of the maximum stress in terms of non-homogenous index (*n*)

Fig. 8 The distribution of the maximum electric potential in terms of non homogenous index (*n*)

direction (*y*) at *x* = 0.1. Fig. 10 shows the distribution of the electric potential for six values of the non homogenous index at *x* = 0.05.

3.2.1 Linear analysis, comparison with nonlinear responses

For evaluation of the effect of the geometric nonlinearity on the response of the problem, this section evaluates the linear response of the system. A comprehensive comparison can be done for investigation of the effect of the geometric nonlinearity. A linear analysis is performed by omitting the third term of Eq. (2). The solution procedure for linear analysis can be completed with the same formulations as were presented in section 3.
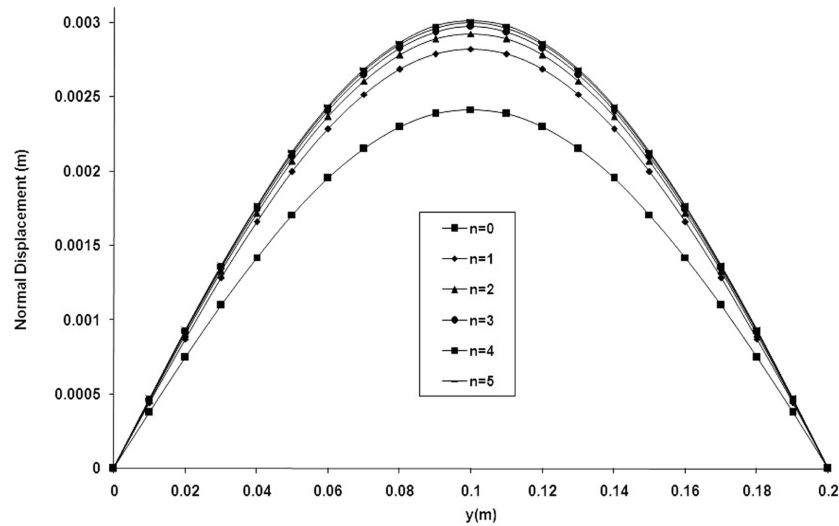
Fig. 9 The distribution of the normal displacement along *y*-axis at *x*=0.1 for 6 values of non homogenous index
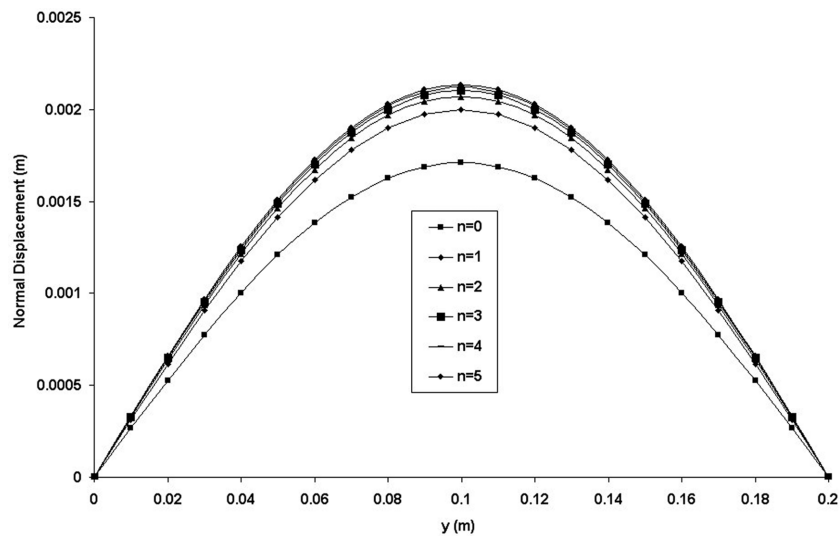

Fig. 10 The distribution of the normal displacement along *y*-axis at *x*=0.05 for 6 values of non-homogenous index (*n*)

Comparison between the nonlinear and linear responses of the maximum normal displacements and electrical potential are shown in Figs. 11, 12 for different non-homogenous indexes (*n*).

3.2.2 Comparison between the present results with a FG square plate

The present results can be compared with those results that are obtained for a FG square plate composed of FGM of exponential law (GhannadPour and Alinia 2006, Alinia and
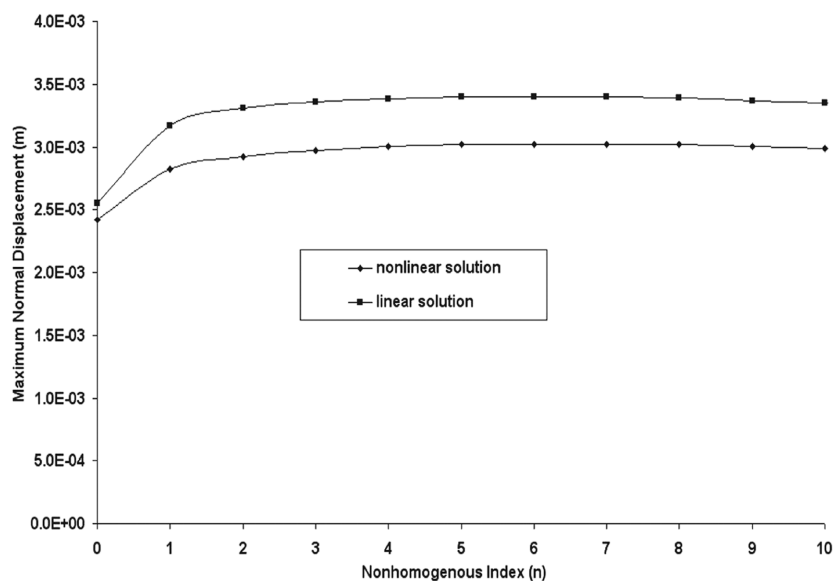
Fig. 11 The comparison between the nonlinear and linear responses (maximum normal displacement)
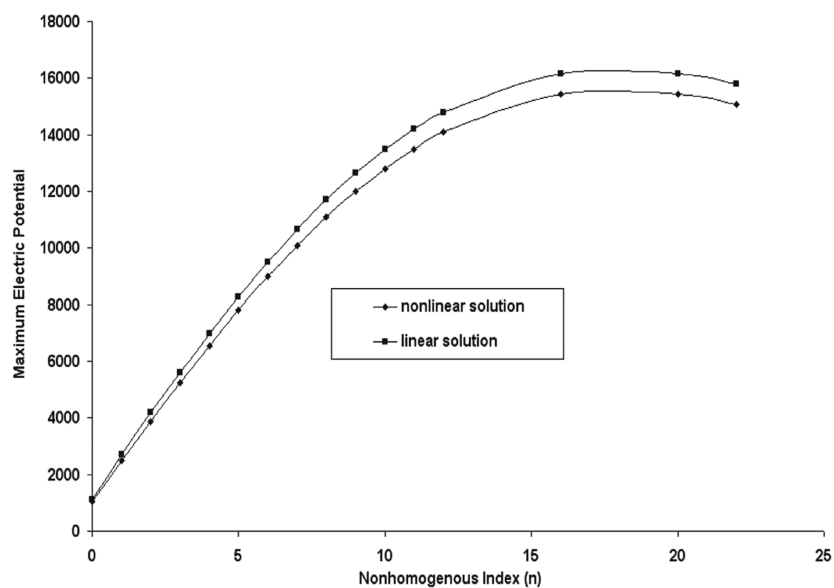

Fig. 12 Comparison between the nonlinear and linear responses (maximum electric potential)

GhannadPour 2009). By disregarding the two smart layers of the FGP square plate and equaling the geometric dimensions and mechanical properties, a comprehensive comparison can be presented. Fig. 13 shows this comparison (GhannadPour and Alinia 2006, Alinia and GhannadPour 2009).
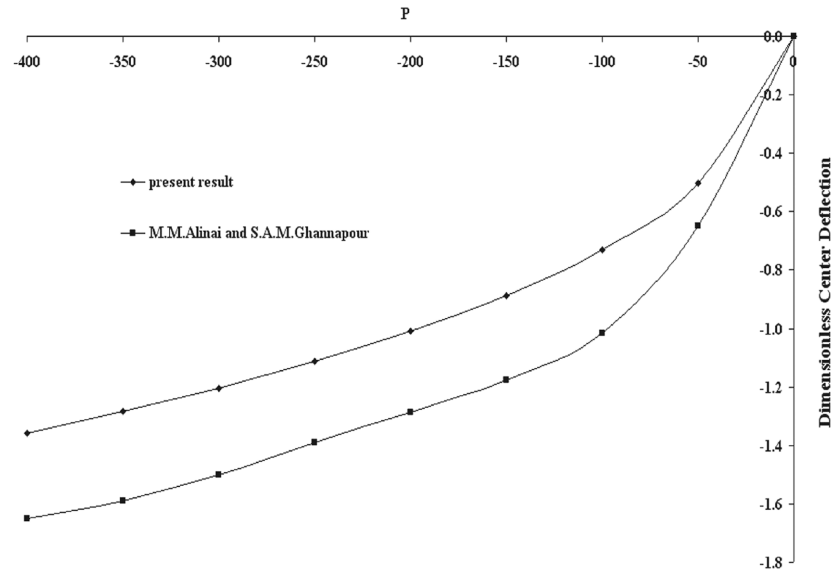
Fig. 13 The comparison between the results of a FGP square plate in a special case with a FG square plate

4. Conclusions

Nonlinear analysis of the pressurized FGP square plate was investigated analytically in this work. The plate was composed of a FG layer and two smart FGP layers at top and bottom of that. The geometric nonlinearity was considered in the strain-displacement relation. Following conclusions can be regarded:

1. This paper presents an accurate and adjustable tool for analysis of the measurement instruments such as sensors. The nonlinear analysis increases the accuracy of experimental data that are extracted from the measurement instruments with respect to a linear analysis. Displacement-pressure and potential-pressure curves verify the nonlinearity of the problem.

2. Distribution of the displacement, stress and electric potential in terms of the non-homogenous index indicates that with increasing the non-homogenous index, the mechanical and electrical components such as displacement and electric potential tend to an asymptotic value.

3. A linear analysis is done and the obtained results are compared with those results that are extracted from the nonlinear analysis. This comparison indicates that the effect of geometric nonlinearity must be regarded in the analysis of FGP structures especially for measurement instruments such as sensor.

4. The obtained results for a FGP square plate can be compared with a FG square plate with exponential law of material properties (GhannadPour and Alinia 2006, Alinia and GhannadPour 2009). If we disregard the piezoelectric layers of cylinder at top and bottom, the present results can be compared with literature.

References

Alinia, M.M. and Ghannadpour, S.A.M. (2009), "Nonlinear analysis of pressure loaded FGM plates", *Compos. Struct.*, **88**(3), 354-359.

Allahverdizadeh, A., Naei, M.H. and Nikkhah Bahrami, M. (2008), "Vibration amplitude and thermal effects on the nonlinear behavior of thin circular functionally graded plates", *Int. J. Mech. Sci.*, **50**(3), 445-454.

Allahverdizadeh, A., Naei, M.H. and Nikkhah Bahrami, M. (2008), "Nonlinear free and forced vibration analysis of thin circular functionally graded plates", *J. Sound. Vib.*, **310**(4-5), 966-984.

Banerjee, A., Bhattacharya, B. and Mallik, A.K. (2008), "Large deflection of cantilever beams with geometric nonlinearity: Analytical and numerical approaches", *Int. J. Nonlinear Mech.*, **43**(5), 366-376.

Boresi, A. (1993), *Advanced mechanics of materials*, John wiley & sons.

Ebrahimi, F. and Rastgo, A. (2008), "An analytical study on the free vibration of smart circular thin FGM plate based on classical plate theory", *Thin. Wall. Struct.*, **46**(12), 1402-1408.

GhannadPour, S.A.M. and Alinia, M.M. (2006), "Large deflection behavior of functionally graded plates under pressure loads", *Compos. Struct.*, **75**(1-4), 67-71.

Hui-Shen, S. (2007), "Nonlinear thermal bending response of FGM plates due to heat conduction", *Compos. Part. B-Eng.*, **38**(2), 201-215.

Khoshgoftar, M.J., Ghorbanpour Arani, A. and Arefi, M. (2009) "Thermoelastic analysis of a thick walled cylinder made of functionally graded piezoelectric material", *Smart. Mater. Struct.*, **18**(11), 115007.

Lai, M. Rubin, D. and Krempl, E. (1999), *Introduction to continuum mechanics*, Buttenvorth-Heinemann.

Malekzadeh, P. and Vosoughi, A.R. (2009), "DQM large amplitude vibration of composite beams on nonlinear elastic foundations with restrained edges", *Commun. Nonlin. Sci. Num. Sim.*, **14**(3), 906-915.

Olfatnia, M., Xu, T., Miao, J.M., Ong, L.S., Jing, X.M. and Norford, L. (2010), "Piezoelectric circular microdiaphragm based pressure sensors", *Sensor. Actuat. A - Phys.*, **163**(1), 32-36

Rahimi, G.H., Arefi, M. and Khoshgoftar, M.J. (2011), "Application and analysis of functionally graded piezoelectrical rotating cylinder as mechanical sensor subjected to pressure and thermal loads", *Appl Math Mech - Engl Ed.*, **32**(8), 1-12.

Sarfaraz Khabbaz, R., Dehghan Manshadi, B. and Abedian, A. (2009), "Non-linear analysis of FGM plates under pressure loads using the higher-order shear deformation theories", *Compos. Struct.*, **89**(3), 333-344.

Soufyane, A. (2009), "Exponential stability of the linearized non uniform Timoshenko beam", *Nonlinear. Anal - Real.*, **10**, 1016-1020.

Ugural, A.C. (1981), *Stress in plate and shells*, McGraw-Hill.

Woo, J. and Meguid, S.A. (2001), "Nonlinear analysis of functionally graded plates and shallow shells", *Int. J. Solids. Struct.*, **38**(42-43), 7409-7421.

Zy kaa, P. and Janus, P. (2010), "Applicability of MEMS cantilever micro-dilatometer for direct transverse strain monitoring in electroactive polymers", *Sensor. Actuat. A - Phys.*, **163**(1), 111-117.

CC

Nomenclature

C_{ijkl}	: stiffness coefficient
C_{ijkl}^{e}	: stiffness coefficient for FG layer
C_{ijkl}^{p}	: stiffness coefficient for FGP layer
D_i	: electric potential
e_{ijk}	: piezoelectric coefficient
E_k	: electric field components
$2h_e$	: thickness of FG layer
h_p	: thickness of FGP layer
L	: length of the square plate
p	: applied pressure
$E(z)$	: distribution of material properties
x, y, z	: components of coordinate system
u, v, w	: displacement components at a general point
u_0, v_0, w	: displacement components at midplane
ε_{ij}	: strain components

σ_{ij} : stress components
$\bar{u}$: energy per unit volume
U : total energy of system
η_{ik} : dielectric coefficient
$U_{mn}, V_{mn}, W_{mn}, \Phi_{mn}$: amplitude of assumed function
ϕ : electric potential
p, q : the number of terms for displacement and electric field
n : non-homogenous index